ACS OMEGA

http://pubs.acs.org/journal/acsodf

Article

Utilization of Antibody Allows Rapid Clearance of Nanoparticle Probes from Blood without the Need of Probe Modifications

Akira Makino,* Hidehiko Okazawa, and Yasushi Kiyono

Cite This: *ACS Omega* 2021, 6, 21153−21159

Read Online

ACCESS | Metrics & More | Article Recommendations | Supporting Information

ABSTRACT: Nanoparticles are attracting attention as drug carriers for realizing "theranostics". However, nanoparticles generally show long blood circulation behaviors, and the remaining nanoparticle probe in the blood is the cause of prolonged optimal time from probe injection to imaging. Recently, it has been reported that some nanoparticles activate the immune system, producing an anti-nanoparticle antibody, which can selectively detect the corresponding nanoparticle and transfer it to the liver by opsonization. Lactosome is a polymer micelle prepared from amphiphilic PNMG-*block*-PLLA polydepsipeptide and known to activate the immune system when administered to mice at a specific concentration. In this study, radioactive fluorine-labeled lactosome (^{18}F-lactosome) is used as a positron emission tomography probe for tumor imaging, and anti-lactosome antibody was additionally administrated after 2 h from the probe dosage. ^{18}F-lactosome remaining in the blood was opsonized by the anti-lactosome antibody and transferred to the liver under the antibody dose-dependent manner. Because of the probe reduction from the blood, the tumor/blood signal intensity ratio could be improved up to 50% by anti-lactosome antibody administration. There needs further improvement, but the developed method is applicable for imaging utilizing nanoparticle probes, which activate the immune system.

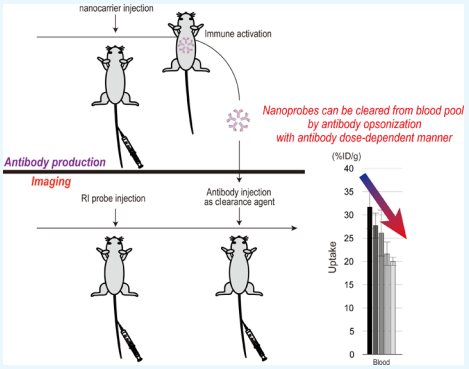

INTRODUCTION

Nuclear imaging is one of the powerful methods for non-invasive functional imaging because of its high sensitivity and the ability to image deep inside the body. Various imaging probes visualizing glucose metabolism, cell growth, and specific receptors on target cells have been developed and clinically utilized.[1−3]

Nano-sized particles such as polymer micelles can encapsulate any compounds, and their utilizations as carriers for drug delivery systems have been actively investigated. Nanoparticles are known to be passively accumulated in the tumor region by the enhanced permeability and retention effect[4,5] and also apply to active targeting by their surface modification with ligands such as peptides and antibodies, which can bind with receptors highly expressed on the target cells.[6] Therefore, by encapsulation or chemical labeling of signal compounds such as fluorescein dyes, radioisotopes, and so forth to nanoparticle carriers, they can also utilize as imaging probes. Another important characteristic of molecular assembling nanoparticles such as polymer micelle is a relatively easy preparation process. Surface-modified micelle can be quickly prepared by only mixing appropriate preliminary designed micelle components.[7,8] Especially in the field of nuclear medicine, this quick and simple preparation process is essential for future clinical applications from the viewpoint of radionuclide half-life and avoiding radiation exposure of chemists during preparations. Therefore, nanoparticles are expected as a key material for realization of "theranostics", which is aiming for seamless diagnosis and treatment.[9−14]

On the other hand, most of the nanoparticle carriers developed are covered with hydrophilic polymers such as polyethylene glycol so as not to be recognized by reticuloendothelial systems and excrete from the body, which causes for the nanoparticle long-lasting blood circulation behaviors.[15] For the treatment drug delivery, this long-lasting blood circulation behavior contributes to maintaining the drug concentration in blood high enough for the treatment. However, on imaging, a strong signal derived from the nanoparticle probe remaining in the blood becomes noise for images. Therefore, it is favorable to wait until probes circulating in blood are excreted from the body, which causes prolonged adequate time from probe administration to imaging.[16,17] Because of the radionuclide half-life, administration of an excess amount of radiation probes or utilization of longer half-life radionuclides such as ^{64}Cu, whose half-life is 12.7 h, is essential to obtain clear images using nanoparticle probes by positron emission tomography (PET). In order to

Received: June 11, 2021
Accepted: July 26, 2021
Published: August 5, 2021

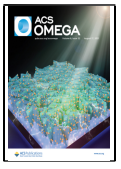

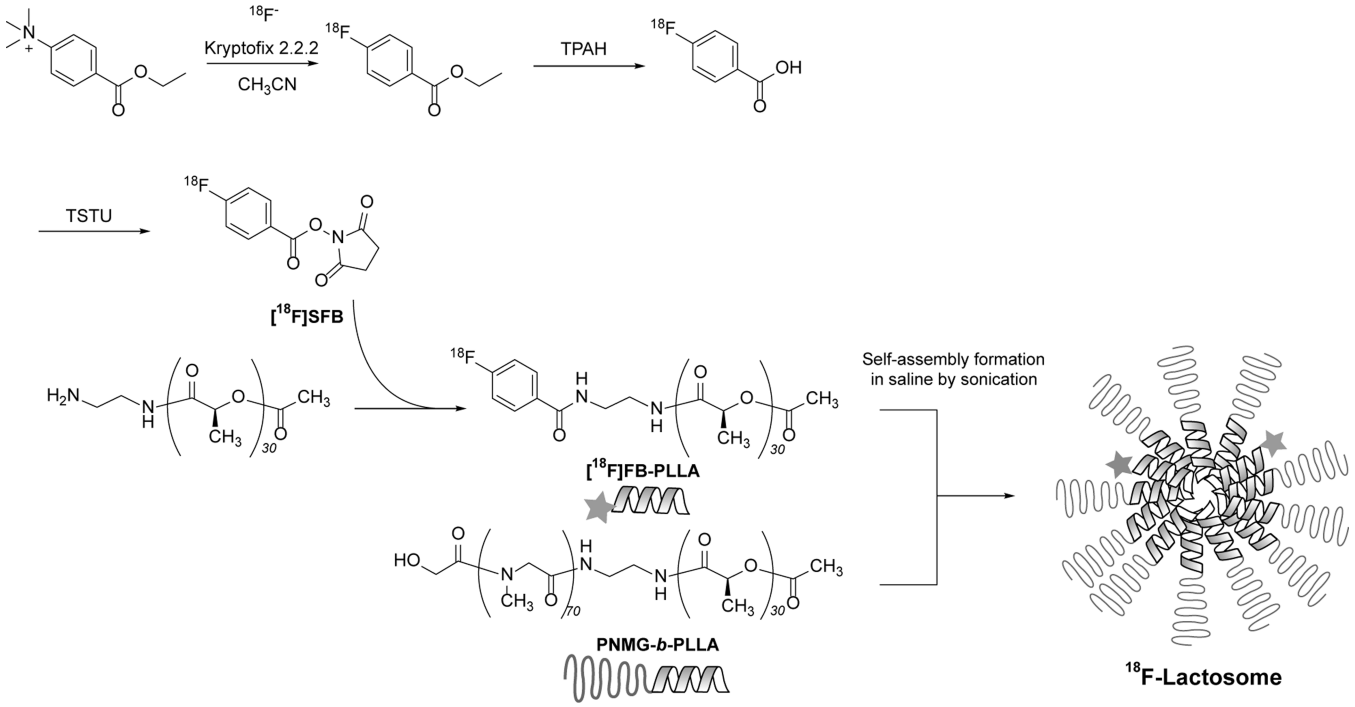

Figure 1. Preparation of ^{18}F-lactosome using succinimidyl-[^{18}F]fluorobenzoate ([^{18}F]SFB) method.

reduce the undesired exposure of patients and imaging technicians, reducing the adequate time from probe administration to imaging is one of the important approaches.

In 1990s, several attempts were performed to remove nanoparticles in blood using a clearance agent.[18−20] In these papers, biotin−avidin binding, which is a representative strong and specific protein−ligand interaction, was used. Liposomes, whose surface was modified with biotin, could be removed from the blood pool by following avidin solution administration as a clearance agent. However, application examples of the system are limited. This may be because amount of avidin needed for the liposome removal is high. For adaptation of the biotin−avidin system to nanoparticles, there needs their surface modification with biotin, which can also lead to undesired pharmacokinetic and/or stability changes.

Recently, it is revealed that some nanoparticles activate the immune system under specific conditions and the corresponding anti-nanoparticle antibody (IgM) is produced, which is called as the accelerated blood clearance (ABC) phenomenon.[21−23] There still leave many unrevealed points, for example, how to active the immune system, which structure is worked as antigen, and so on. However, the important thing is that the antibody can selectively detect and remove the corresponding nanoparticle from the blood pool by opsonization without any nanoparticle surface modification such as the biotin−avidin system.

Lactosome is a polymer micelle prepared from poly(*N*-methylglycine)-*block*-poly(L-lactic acid) (PNMG-*b*-PLLA),[16] and its utilization has been reported as carriers for tumor nuclear imaging[24] and therapeutic drugs. It is also reported that a mouse immune system is activated by lactosome administration, producing anti-lactosome antibodies (IgM and IgG_3).[25] The lactosome ABC phenomenon has been well evaluated, and the dose needed for the immune system activation was also reported. Therefore, we selected lactosome as a model nanoparticle for evaluating the effect of anti-nanoparticle antibody as a clearance agent in this study. The purpose of this study is to develop a method for background signal reduction derived from nanoparticle probes in blood, which is applicable to arbitrary nanoparticles producing corresponding anti-nanoparticle antibody including liposomes. This basic methodology is applicable to not only nuclear imaging but also various kinds of imaging techniques using probes such as near-infrared fluorescein, magnetic resonance, and so on.

RESULTS

Radioisotope-Labeled PLLA Syntheses and Polymeric Micelle (Lactosome) Preparations. As positron-emitting radionuclides, fluorine-18 whose half-life is ca. 109.8 min and widely utilized for PET imaging was selected. The preparation of radioisotope-labeled lactosome is shown in Figure 1. Polymers used for the experiments were synthesized according to the papers previously reported.[16] The ^{1}H NMR spectra of H_2N-PLLA and PNMG-*b*-PLLA are shown in the Supporting Information (Figure S1). Succinimidyl [^{18}F]fluorobenzoate ([^{18}F]SFB) was reacted to the primary amine, which is inserted at the terminal end of PLLA 30 mer (H_2N-PLLA). The resulting ^{18}F-labeled PLLA ([^{18}F]FB-PLLA) was purified by size exclusion chromatography, and the radiochemical yield was 32.1%.

^{18}F-labeled micelle (^{18}F-lactosome) preparation was performed by a film rehydration method, indicating that saline was added to the mixture of PNMG-*b*-PLLA and [^{18}F]FB-PLLA and sonicated at 90 °C for 5 min. The micelles prepared were purified by size exclusion chromatography and used for the following experiments (Figure S2). Radioactivity was only detected from fractions containing polymer micelles. Encapsulation rate of [^{18}F]FB-PLLA into the micelle was 97.7%, which was determined by calculation by dividing radioactivity in micelle factions by that bedded on the column. A non-radioisotope-labeled polymeric micelle (lactosome) was

https://doi.org/10.1021/acsomega.1c03076
ACS Omega 2021, 6, 21153−21159

prepared from PNMG-*b*-PLLA by the same preparation method. The diameter and ζ-potential of ^{18}F-lactosome and lactosome were 41.7 ± 0.4 and 40.8 ± 0.1 nm, −3.05 ± 0.25 and −3.18 ± 0.20 mV, respectively, which showed no significant difference. Further, spherical micelle formation was confirmed by transmission electron microscopy (TEM) observations (Figure S3).

Preparation of Blood Serum Containing Anti-lactosome Antibody. Polymer micelle (lactosome) solution was intravenously injected to the mice. As reported previously, the amount of anti-lactosome antibody in blood reaches maximum on day 5 and remains high at least up to day 14.[25] Therefore, in this study, mice were sacrificed after 7 days from the administration, and blood was collected. The following day, blood serum was collected. Part of the pooled serum was condensed by ultrafiltration, and the relative anti-lactosome IgM amount in the serum was analyzed by ELISA (Figure 2).

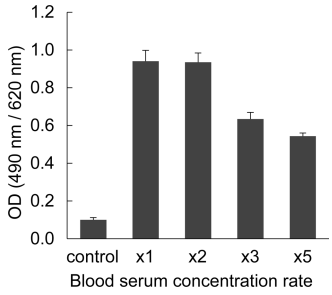

Figure 2. Relative amount of anti-lactosome IgM after 7 days from lactosome (5 mg/kg) dosage. Serum from mice without lactosome injection was used as a control. x1 indicates original serum, and x2−x5 shows the concentration rate. The condensed serum (x2−x5) was diluted by PBS to the original concentration just before the ELISA assay. The data is the average value of three measurements.

ELISA assay was carried out after dilution by phosphate-buffered saline (PBS) to the original concentration, and abbreviations x1 and x2−x5 mean original serum and their concentration rates, respectively. The anti-lactosome IgM activity was declined when the serum was condensed more than three times.

Effect of Anti-lactosome Antibody Injection on the Micelle Pharmacokinetics. As illustrated in Figure 3a, the ^{18}F-labeled polymer micelle (^{18}F-lactosome) was intravenously injected to the mice from the tail vein. Since the half-life of fluorine-18 is 109.8 min, we decided to administrate the antibody after 2 h from the ^{18}F-lactosome injection. Indeed, various concentrations of anti-lactosome IgM containing serum-based solution (100 μL) was then i.v. injected, whose concentration was adjusted using PBS. The anti-lactosome IgM titers injected per mice were 0.21, 0.42, 0.84, and 1.67. As a control, PBS (100 μL) was injected. The mice were sacrificed at 15 min from the second administration, and ^{18}F biodistribution was evaluated by the organ harvesting method. Blood serum condensed more than 3-folds were not used for *in vivo* study because of the lowered anti-lactosome IgM activity (Figure 2) and increased solution viscosity (data not shown). ^{18}F activity detected from blood was the second dose dependently decreased, oppositely that from liver was increased (Figure 3b). Additionally, biodistribution data when the mice were sacrificed after 30 min from the second anti-lactosome IgM administration, whose titer is of 0.84 (100 μL), was shown in Figure 3b (0.84; 30 min). No significant difference was observed on ^{18}F biodistribution due to the time difference from the second antibody administration to the evaluation time (0.84 and 0.84; 30 min).

Figure 4 shows the relationship between the amount of anti-lactosome IgM injected to mice and ^{18}F-lactosome uptake in (a) blood and (b) liver. The ^{18}F activity reduction in blood and increase in liver were both well linearly correlated with the injected anti-lactosome IgM doses, whose R^2 values were 0.85 and 0.97, respectively.

Effect of Anti-lactosome Antibody Injection on Tumor Imaging. ^{18}F-lactosome was intravenously injected to the tumor-bearing mice. At 2 h from the first dosage, condensed blood serum solution containing anti-lactosome IgM whose titer was 1.67 (100 μL) or PBS (control, 100 μL) was injected. After 15 min from the second administration, the mice were sacrificed and the ^{18}F biodistribution was evaluated (Table 1). The ^{18}F activity in blood was significantly decreased from 39.14 ± 0.54 to 27.90 ± 4.76% ID/g and that in liver was increased from 8.78 ± 2.23 to 15.50 ± 0.90% ID/g. However, those at other organs including tumor were not changed significantly. Change of tumor/blood ^{18}F intensity ratio was from 0.046 ± 0.009 to 0.068 ± 0.019.

DISCUSSION

In this study, two types of polymer micelles, indeed, ^{18}F-labeled (^{18}F-lactosome) and non-radioisotope-labeled (lactosome) micelles, were prepared. These two micelles show no significant difference on micelle diameter, ζ-potential, and shapes. This might be because the amount of [^{18}F]FB-PLLA mixed into PNMG-*b*-PLLA for radioisotope labeling was ca. 7.7 wt %, which is not high enough to affect the micelle assembling. Further, hydrophobic [^{18}F]FB-PLLA is encapsulated into the core region of the micelle and shielded by the shell region consisted by hydrophilic PNMG moieties.

For the high-contrast tumor imaging, improving the probe accumulation to the target and/or decreasing the background signal from untargeted regions are essential. As shown in Figure 3, the undesired ^{18}F activity from blood could be decreased up to 30% by blood serum administration containing anti-lactosome IgM as a clearance agent. This is because ^{18}F-lactosome remaining in the blood pool is opsonized by anti-lactosome IgM in the serum and trapped by reticuloendothelial systems such as liver and spleen. The ^{18}F activity reduction in blood and the increase in liver were both well linearly correlated with the injected anti-lactosome IgM doses (Figure 4), but the ^{18}F activity detected from other organs showed no significant differences. These results support that the opsonization occurred in the blood pool and the opsonized micelle was mainly trapped by liver. The ^{18}F distribution after 15 and 30 min from the blood serum administration showed no significant difference (Figure 3b), indicating the micelle opsonization, and antibody removal from the blood pool quickly occurred soon after the second antibody administration. Further, since nanoparticles removed from blood were accumulated in the liver, it is preferable that this method should be applicated to imaging, targeting a site distant from the liver.

In Figure 4a, the relative amount of the anti-lactosome IgM value 1.67 corresponds 2-fold condensed serum was administrated to mice. If this 2-fold condensed serum data is excluded, the ^{18}F activity in blood showed higher linear correlation (R^2 = 0.97) with the anti-lactosome IgM amount. This may be due to the increased serum viscosity by

https://doi.org/10.1021/acsomega.1c03076
ACS Omega 2021, 6, 21153−21159

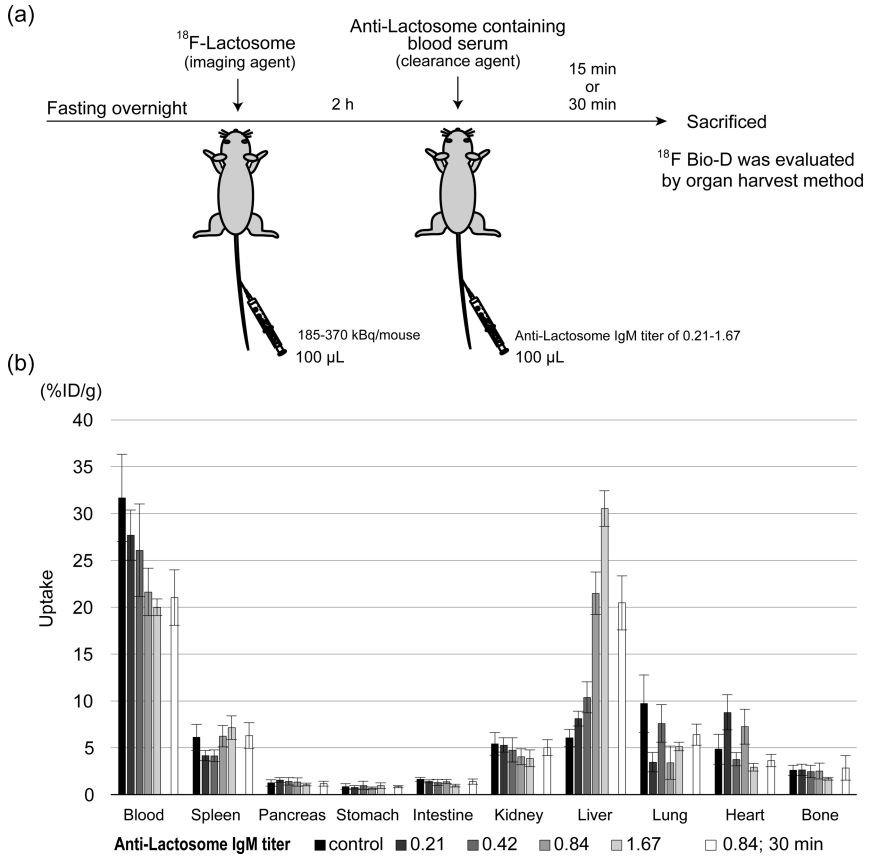

Figure 3. (a) Schematic diagram of the *in vivo* experiment. (b) Biodstribution of ^{18}F-lactosome after 15 min from intravenous serum (100 μL) administration containing anti-lactosome antibody. As a control, PBS was used. The blood serum was diluted by PBS so as the injection volume becomes 100 μL. An anti-lactosome titer of 0.84 serum as it was, and 1.67 was a 2-fold condensed serum by ultrafiltration. 0.84; 30 min indicates the biodistribution date after 30 min from the second administration. The data are an average of n = 3 mice.

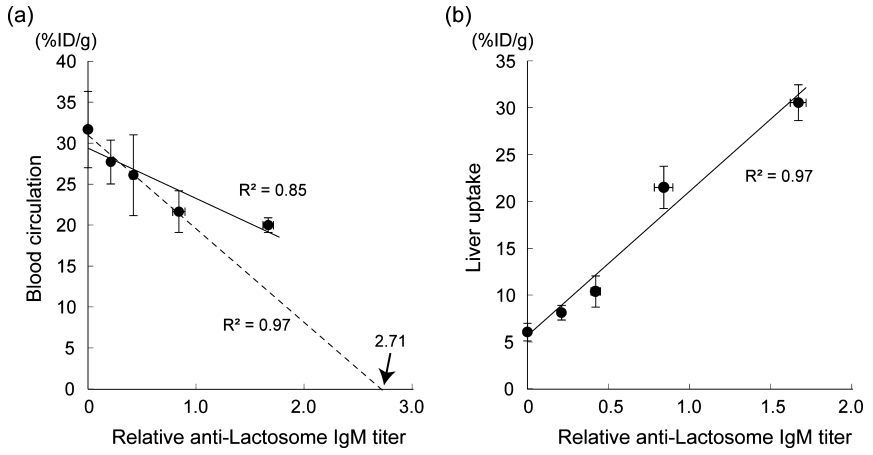

Figure 4. Relationship between the amount of anti-lactosome IgM injected to mice and (a) blood and (b) liver uptake. The amount of injected anti-lactosome IgM was calculated as follows: (injected anti-lactosome IgM) = (OD value shown in Figure 2) × (injected original blood serum volume (μL)/100) − (control OD value).

condensation, which changes antibody pharmacokinetics and decreases the micelle removal efficiency. Using the linear approximation excluding condensed serum (dash-line in Figure 4a), the needed anti-lactosome IgM titer removing all lactosome in blood is simply calculated to be 2.71, which is equivalent to the blood serum (320 μL) in this study. The volume is too much to administrate at one time to mice. As descried previously, the blood serum condensed over 3-folds by ultrafiltration leads to antibody deactivation (Figure 2), and the solution viscosity increases, which are not suitable for the administration. The cause of antibody titer decrease is unclear, but purification of the antibody is essential for the dosage.

On ^{18}F-lactosome tumor imaging, it was reported that the tumor/blood radioactivity intensity ratio is slowly improved because of the gradual accumulation of lactosome at the tumor and elimination from blood, and those at 2, 4, and 6 h from the administration was 0.05 ± 0.01, 0.07 ± 0.01, and 0.09 ± 0.00%, respectively.[24] Considering the ^{18}F half-life (109.8 min)

https://doi.org/10.1021/acsomega.1c03076
ACS Omega 2021, 6, 21153−21159

Table 1. Effect on ^{18}F-Lactosome Biodistribution by Anti-lactosome IgM Administration to Tumor-Bearing Mice (n = 3)[a]

tissue	control (PBS) (% ID/g)	anti-lactosome IgM (% ID/g)	significant difference
blood	39.14 ± 0.54	27.87 ± 4.76	$p < 0.05$
spleen	8.78 ± 1.92	10.55 ± 1.73	n.s.
pancreas	1.42 ± 0.02	1.92 ± 0.34	n.s.
stomach	1.60 ± 0.20	1.96 ± 0.53	n.s.
intestine	1.56 ± 0.22	1.85 ± 0.31	n.s.
kidney	6.29 ± 0.18	5.56 ± 2.29	n.s.
liver	8.78 ± 2.23	15.50 ± 0.90	$p < 0.05$
lung	9.80 ± 0.75	9.42 ± 1.02	n.s.
heart	4.53 ± 0.92	4.95 ± 0.79	n.s.
tumor	1.80 ± 0.39	1.84 ± 0.17	n.s.
muscle	0.88 ± 0.12	0.82 ± 0.07	n.s.
bone	2.17 ± 0.37	1.65 ± 0.35	n.s.
tumor/muscle	2.02 ± 0.17	2.25 ± 0.04	n.s.
tumor/blood	0.046 ± 0.009	0.068 ± 0.019	n.s.

[a]Significant differences between the two groups were evaluated using the Bonferroni−Dunn method.

and ^{18}F-lactosome biodistribution data, the serum injection time as a clearance agent was set to be 2 h from the first ^{18}F-lactosome injection in this study. As a clearance agent, an anti-lactosome IgM titer of 1.67 serum solution, which is currently expected to be the most effective, was used. The improved tumor/blood ^{18}F intensity ratio from 0.046 ± 0.009 to 0.068 ± 0.019 is derived from the 30% decrease of ^{18}F-lactosome circulating in blood. This result shows that the tumor/blood signal intensity ratio (0.07), which normally requires 4 h waiting, can be achieved after 2 h (0.068) by using the antibody as a clearance agent. However, because the radioactivity present in the blood pool is still larger than that accumulated in tumor region and the influence of individual differences, improvement tendency of tumor/blood signal intensity ratio could be confirmed but not found significant difference, statistically.

In order to improve the tumor/blood ratio value over 1, more than 90% of ^{18}F-lactosome should be removed from the blood pool by calculation. Increased antibody dosage by anti-lactosome IgM purification is a considerable approach. Another solution is to reduce the remaining ^{18}F-lactosome in blood. Because of the ^{18}F-lactosome preparation process, the ^{18}F-lactosome specific activity used in this study was not high and the calculated micelle dose per mice reached to 1.5−2.0 mg. If the ^{18}F-lactosome specific activity can be improved 10 times and the lactosome dose can be reduced to 1/10, ^{18}F-lactosome remaining in blood will be able to remove sufficiently by the current antibody dose.

Although there still need developments, these results clearly show that the image contrast could be improved by anti-lactosome antibody administration as a clearance agent.

CONCLUSIONS

In this study, the effect of anti-nanoparticle antibody as a clearance agent was evaluated using lactosome as a polymeric micelle model. Lactosome circulating in the blood pool can be removed by anti-lactosome antibody with a dose-dependent manner. To improve the tumor/blood intensity ratio more, there needs complete removal of nanoparticle probes from blood. They are still left to be improved, but utilizing an anti-nanoparticle antibody as a clearance agent is an effective approach to shorten the time from nanoparticle probe administration to imaging.

MATERIALS AND METHODS

Chemistry. All chemical regents and solvents were purchased from commercial sources and used without further purifications. The ^{1}H NMR spectra were recorded on a JEOL ECX-500II spectrometer (Tokyo, Japan) with TMS as an internal standard. Purification was performed using a Prominence high-performance liquid chromatography (HPLC) system (Shimadzu Corp., Kyoto, Japan) equipped with Cosmosil 5C18-AR-II (4.6 × 150 mm, Nacalai Tesque, Kyoto, Japan) or Shodex Asahipak GF-310HQ (7.5 × 300 mm, Showa Denko K. K., Tokyo, Japan) columns. As the mobile phase, acetonitrile/H_2O containing 0.1% trifluoroacetic acid (AR-II) and acetonitrile (GF-310) were used at a flow rate of 1.0 and 0.5 mL/min, respectively.

Preparation of 4-[^{18}F]fluorobenzyl-PLLA ([^{18}F]FB-PLLA). Fluorine-18 was synthesized by the (p, n) reaction from ^{18}O enriched water (Taiyo Nippon Sanso Corp. Tokyo, Japan) using an Eclipse Cyclotron system (Siemens, Munich, Germany). Succinimidyl [^{18}F]fluorobenzoate ([^{18}F]SFB) was synthesized as a previously reported method using a Hybrid automatic synthesizer (JFE Engineering Corp. Tokyo, Japan).

To the [^{18}F]SFB vial, a primary amino group bearing PLLA 30 mer 1.5 mg (H_2N-PLLA) dissolved in dimethyl sulfoxide (150 μL) and a portion of triethylamine were added. The mixture was heated at 100 °C for 20 min under shaking and then purified using an HPLC (Prominence) system (Shimadzu Corp. Kyoto, Japan) equipped with a Shodex Asahipak GF-310HQ. The radiochemical yield of [^{18}F]FB-PLLA was 32.1% EOB (total synthetic time: 27 min).

Polymer Micelle Preparation. The polymer micelle was prepared using a polymer film rehydration method. PNMG-*b*-PLLA (2.0 mg) dissolved in chloroform (0.50 mL) was added into the test tube, and the polymer film was formed by evaporation. To the test tube, PBS at pH 7.4 (1.0 mL) was added, and the mixture was sonicated at 80 °C using a bath-type sonicator. Radiolabeled micelle (^{18}F-lactosome) was prepared starting from the mixture of PNMG-*b*-PLLA (18 mg) and [^{18}F]FB-PLLA (1.5 mg). The micelle solutions were purified by a PD-10 prepacked column (Cytiva, MA, USA). The obtained solution was passed through a 0.8 μm membrane filter (Pall Corp., NY, USA) before use. The diameter of the micelle and the ζ-potential were determined by the dynamic light scattering method using a Zetasizer Nano ZSP (Malvern Panalytical, Malvern, UK).

Animals. All of our *in vivo* experiments were approved by the Animal Research Committee of University of Fukui. All animals were socially housed under environmentally controlled conditions (12 h normal light/dark cycles, 22−24 °C, and 40−50% relative humidity) with food and water ad libitum. Isoflurane inhalation anesthesia was used for micelle administration and blood collection. The authors confirm that all applicable institutional guidelines for the care and use of animals were followed.

Preparation of Blood Serum Containing Anti-lactosome Antibody. The micelle solution (100 μL) was intravenously injected to the 8 week-old male ddY mice (Japan SLC Inc., Hamamatsu, Japan). The micelle dosage was set to be 5 mg/kg. At 7 days post-injection, the mice were anesthetized, and blood was collected through cardiac

https://doi.org/10.1021/acsomega.1c03076
ACS Omega 2021, 6, 21153−21159

puncture. The blood was kept at 4 °C for 16 h, and then plasma was obtained by centrifugation (1000*g*, 4 °C, 25 min). The collected blood serum was stored at −80 °C. Blood serum condensation was performed using Amicon Ultra 30K centrifugal filters (MilliporeSigma, Burlington, USA).

The relative amount of anti-lactosome IgM in the serum was evaluated by the ELISA assay as previously reported.[25] The condensed serum was diluted by PBS to the original concentration before the measurement. Peroxidase-conjugated goat-anti-mouse IgM in 0.1% bovine serum albumin/PBS (SouthernBiotech, AL, USA) was used. The UV absorbance ratio at (490/620 nm) was measured by SpectraMax (Molecular Devices, CA, USA).

Biodistribution Study. In this study, a number of mice in each group was set to be $n = 3$. To the 8 week-old male ddY mice, radiolabeled micelle PBS solution (185−370 kBq, 100 μL) was intravenously administrated. At 2 h post-administration, anti-lactosome IgM containing serum (100 μL) was injected as a clearance agent. After 15 or 30 min from the second administration, the mice were sacrificed and ^{18}F distribution was evaluated by an organ harvesting method. Radioactivity was measured by a Wallac 1480 gamma counter (PerkinElmer, MA, USA), and the accumulation amount was standardized by the weight of each organ and injected dose (ID) of the radioactivity (% ID/g).

As a tumor model, an FM3A cell (5×10^6) (RIKEN BRC, Tsukuba, Japan) was transplanted to the right femoral region of BALB/c nu−nu mice (8 weeks). An *in vivo* study was performed after 14 days from the transplantation.

■ ASSOCIATED CONTENT

Supporting Information

The Supporting Information is available free of charge at https://pubs.acs.org/doi/10.1021/acsomega.1c03076.

Chart of size exclusion chromatography and TEM images (PDF)

■ AUTHOR INFORMATION

Corresponding Author

Akira Makino − *Biomedical Imaging Research Center, University of Fukui, Fukui 910-1193, Japan; Life Science Innovation Center, University of Fukui, Fukui 910-8507, Japan;* orcid.org/0000-0003-1381-5586; Email: amakino@u-fukui.ac.jp

Authors

Hidehiko Okazawa − *Biomedical Imaging Research Center, University of Fukui, Fukui 910-1193, Japan; Life Science Innovation Center, University of Fukui, Fukui 910-8507, Japan*

Yasushi Kiyono − *Biomedical Imaging Research Center, University of Fukui, Fukui 910-1193, Japan; Life Science Innovation Center, University of Fukui, Fukui 910-8507, Japan*

Complete contact information is available at: https://pubs.acs.org/10.1021/acsomega.1c03076

Author Contributions

A.M., H.O., and Y.K. participated in the research design. A.M. conducted the experiments and data analysis. A.M. and Y.K. drafted or contributed to the writing of the manuscript. H.O. supervised the experiments.

Funding

This work was supported by the JSPS Grants-in-Aid for Scientific Research grant numbers JP26713040 and JP19K08094.

Notes

The authors declare no competing financial interest.

■ REFERENCES

(1) Been, L. B.; Suurmeijer, A. J. H.; Cobben, D. C. P.; Jager, P. L.; Hoekstra, H. J.; Elsinga, P. H. F-18 FLT-PET in oncology: current status and opportunities. *Eur. J. Nucl. Med. Mol. Imag.* **2004**, *31*, 1659−1672.

(2) Gambhir, S. S. Molecular imaging of cancer with positron emission tomography. *Nat. Rev. Cancer* **2002**, *2*, 683−693.

(3) Pimlott, S. L.; Sutherland, A. Molecular tracers for the PET and SPECT imaging of disease. *Chem. Soc. Rev.* **2011**, *40*, 149−162.

(4) Maeda, H.; Nakamura, H.; Fang, J. The EPR effect for macromolecular drug delivery to solid tumors: Improvement of tumor uptake, lowering of systemic toxicity, and distinct tumor imaging in vivo. *Adv. Drug Deliv. Rev.* **2013**, *65*, 71−79.

(5) Maeda, H.; Wu, J.; Sawa, T.; Matsumura, Y.; Hori, K. Tumor vascular permeability and the EPR effect in macromolecular therapeutics: a review. *J. Controlled Release* **2000**, *65*, 271−284.

(6) Prabhu, R.; Patravale, V. B.; Joshi, M. D. Polymeric nanoparticles for targeted treatment in oncology: current insights. *Int. J. Nanomed.* **2015**, *10*, 1001−1018.

(7) Sethuraman, V. A.; Bae, Y. H. TAT peptide-based micelle system for potential active targeting of anti-cancer agents to acidic solid tumors. *J. Controlled Release* **2007**, *118*, 216−224.

(8) Zhang, L.; Zhu, D. W.; Dong, X.; Sun, H. F.; Song, C. X.; Wang, C.; Kong, D. L. Folate-modified lipid-polymer hybrid nanoparticles for targeted paclitaxel delivery. *Int. J. Nanomed.* **2015**, *10*, 2101−2114.

(9) Chen, G.; Roy, I.; Yang, C.; Prasad, P. N. Nanochemistry and Nanomedicine for Nanoparticle-based Diagnostics and Therapy. *Chem. Rev.* **2016**, *116*, 2826−2885.

(10) Guo, J.; Hong, H.; Chen, G.; Shi, S.; Nayak, T. R.; Theuer, C. P.; Barnhart, T. E.; Cai, W.; Gong, S. Theranostic Unimolecular Micelles Based on Brush-Shaped Amphiphilic Block Copolymers for Tumor-Targeted Drug Delivery and Positron Emission Tomography Imaging. *ACS Appl. Mater. Interfaces* **2014**, *6*, 21769−21779.

(11) Li, Y.; Lin, T. Y.; Luo, Y.; Liu, Q. Q.; Xiao, W. W.; Guo, W. C.; Lac, D.; Zhang, H. Y.; Feng, C. H.; Wachsmann-Hogiu, S.; Walton, J. H.; Cherry, S. R.; Rowland, D. J.; Kukis, D.; Pan, C. X.; Lam, K. S. A smart and versatile theranostic nanomedicine platform based on nanoporphyrin. *Nat. Commun.* **2014**, *5*, 4712.

(12) Pratt, E. C.; Shaffer, T. M.; Grimm, J. Nanoparticles and radiotracers: advances toward radionanomedicine. *Wiley Interdiscip. Rev.: Nanomed. Nanobiotechnol.* **2016**, *8*, 872−890.

(13) Wang, J.; Sang, W.; Yang, Z.; Shen, Z.; Wang, Z.; Jacobson, O.; Chen, Y.; Wang, Y.; Shao, M.; Niu, G.; Dai, Y.; Chen, X. Polyphenol-based nanoplatform for MRI/PET dual-modality imaging guided effective combination chemotherapy. *J. Mater. Chem. B* **2019**, *7*, 5688−5694.

(14) Xiao, Y.; Hong, H.; Javadi, A.; Engle, J. W.; Xu, W.; Yang, Y.; Zhang, Y.; Barnhart, T. E.; Cai, W.; Gong, S. Multifunctional unimolecular micelles for cancer-targeted drug delivery and positron emission tomography imaging. *Biomaterials* **2012**, *33*, 3071−3082.

(15) Blanco, E.; Shen, H.; Ferrari, M. Principles of nanoparticle design for overcoming biological barriers to drug delivery. *Nat. Biotechnol.* **2015**, *33*, 941−951.

(16) Makino, A.; Kizaka-Kondoh, S.; Yamahara, R.; Hara, I.; Kanzaki, T.; Ozeki, E.; Hiraoka, M.; Kimura, S. Near-infrared fluorescence tumor imaging using nanocarrier composed of poly(L-lactic acid)-*block*-poly(sarcosine) amphiphilic polydepsipeptide. *Biomaterials* **2009**, *30*, 5156−5160.

(17) Seo, J. W.; Ang, J.; Mahakian, L. M.; Tam, S.; Fite, B.; Ingham, E. S.; Beyer, J.; Forsayeth, J.; Bankiewicz, K. S.; Xu, T.; Ferrara, K. W.

Self-assembled 20-nm Cu-64-micelles enhance accumulation in rat glioblastoma. *J. Controlled Release* **2015**, *220*, 51−60.
(18) Ogihara-umeda, I.; Sasaki, T.; Nishigori, H. Active removal of radioactivity in the blood-circulation using biotin-bearing liposome and avidin for rapid tumor imaging. *Eur. J. Nucl. Med.* **1993**, *20*, 170−172.
(19) Laverman, P.; Zalipsky, S.; Oyen, W. J.; Dams, E. T.; Storm, G.; Mullah, N.; Corstens, F. H.; Boerman, O. C. Improved imaging of infections by avidin-induced clearance of Tc-99m-biotin-PEG liposomes. *J. Nucl. Med.* **2000**, *41*, 912−918.
(20) van Tilborg, G. A. F.; Strijkers, G. J.; Pouget, E. M.; Reutelingsperger, C. P. M.; Sommerdijk, N. A. J. M.; Nicolay, K.; Mulder, W. J. M. Kinetics of Avidin-Induced Clearance of Biotinylated Bimodal Liposomes for Improved MR Molecular Imaging. *Magn. Reson. Med.* **2008**, *60*, 1444−1456.
(21) Mima, Y.; Hashimoto, Y.; Shimizu, T.; Kiwada, H.; Ishida, T. Anti-PEG IgM Is a Major Contributor to the Accelerated Blood Clearance of Polyethylene Glycol-Conjugated Protein. *Mol. Pharm.* **2015**, *12*, 2429−2435.
(22) Mohamed, M.; Abu Lila, A. S.; Shimizu, T.; Alaaeldin, E.; Hussein, A.; Sarhan, H. A.; Szebeni, J.; Ishida, T. PEGylated liposomes: immunological responses. *Sci. Technol. Adv. Mater.* **2019**, *20*, 710−724.
(23) Shiraishi, K.; Yokoyama, M. Toxicity and immunogenicity concerns related to PEGylated-micelle carrier systems: a review. *Sci. Technol. Adv. Mater.* **2019**, *20*, 324−336.
(24) Yamamoto, F.; Yamahara, R.; Makino, A.; Kurihara, K.; Tsukada, H.; Hara, E.; Hara, I.; Kizaka-Kondoh, S.; Ohkubo, Y.; Ozeki, E.; Kimura, S. Radiosynthesis and initial evaluation of F-18 labeled nanocarrier composed of poly(L-lactic acid)-*block*-poly-(sarcosine) amphiphilic polydepsipeptide. *Nucl. Med. Biol.* **2013**, *40*, 387−394.
(25) Hara, E.; Makino, A.; Kurihara, K.; Yamamoto, F.; Ozeki, E.; Kimura, S. Pharmacokinetic change of nanoparticulate formulation "Lactosome" on multiple administrations. *Int. Immunopharmacol.* **2012**, *14*, 261−266.

https://doi.org/10.1021/acsomega.1c03076
ACS Omega 2021, 6, 21153−21159